HHS Public Access

Author manuscript

*Mucosal Immunol*. Author manuscript; available in PMC 2016 May 18.

Published in final edited form as:

*Mucosal Immunol*. 2016 January ; 9(1): 218–228. doi:10.1038/mi.2015.54.

# Metal-specific CD4+ T cell responses induced by beryllium exposure in HLA-DP2 transgenic mice

**Michael T. Falta, PhD**[1], **Alex N. Tinega**[1], **Douglas G. Mack, PhD**[1], **Natalie A. Bowerman, PhD**[1], **Frances Crawford**[2,3], **John W. Kappler, PhD**[2,3], **Clemencia Pinilla, PhD**[4], and **Andrew P. Fontenot, MD**[1,2]

[1]Department of Medicine, University of Colorado Anschutz Medical Campus, Aurora, CO 80045 USA

[2]Department of Immunology, University of Colorado Anschutz Medical Campus, Aurora, CO 80045 USA

[3]Howard Hughes Medical Institute, National Jewish Health, Denver, CO 80206 USA

[4]Torrey Pines Institute for Molecular Studies, San Diego, CA 92121 USA

## Abstract

Chronic beryllium disease (CBD) is a granulomatous lung disorder that is associated with the accumulation of beryllium (Be)-specific $CD4^+$ T cells into the lung. Genetic susceptibility is linked to *HLA-DPB1* alleles that possess a glutamic acid at position 69 (βGlu69), and *HLA-DPB1*02:01* is the most prevalent βGlu69-containing allele. Using HLA-DP2 transgenic (Tg) mice, we developed a model of CBD that replicates the major features of the human disease. Here, we characterized the T cell receptor repertoire of Be-responsive $CD4^+$ T cells derived from the lungs of Be oxide-exposed HLA-DP2 Tg mice. The majority of Be-specific T cell hybridomas expressed TCR Vβ6, and a subset of these hybridomas expressed identical or nearly identical β-chains that were paired with different α-chains. We delineated mimotopes that bind to HLA-DP2 and form a complex recognized by Be-specific $CD4^+$ T cells in the absence of Be. These Be-independent peptides possess an arginine at p5 and a tryptophan at p7 that surround the Be-binding site within the HLA-DP2 acidic pocket and likely induce charge and conformational changes that mimic those induced by the $Be^{2+}$ cation. Collectively, these data highlight the interplay between peptides and Be in the generation of an adaptive immune response in metal-induced hypersensitivity.

### Keywords

beryllium; granulomatous lung disease; T cell receptor; lung; metals; hypersensitivity



Address correspondence to Dr. Andrew Fontenot, Division of Clinical Immunology (B164), University of Colorado Anschutz Medical Campus, 12700 East 19th Avenue, Aurora, CO 80045; Phone (303) 724-7192; Fax (303) 724-7295; ; Email: andrew.fontenot@ucdenver.edu.

**Disclosure:** The authors have no conflicts of interest to declare.

## INTRODUCTION

Chronic beryllium disease (CBD) is a classic example of a human disorder resulting from gene-by-environment interactions. Genetic susceptibility to CBD is linked to HLA-DP alleles that contain a glutamic acid at the 69th position of the β-chain (βGlu69) ([1]), with the prevalence of βGlu69-expressing HLA-DP alleles ranging from 73-95% of CBD patients ([2-6]). In addition, the probability of CBD increases with HLA-DP βGlu69 copy number and increasing workplace exposure to beryllium (Be) ([7]). Depending on genetic susceptibility and exposure, CBD develops in up to 18% of Be-exposed workers ([1, 8-10]). The disease is characterized by granulomatous inflammation and an influx of Th1-polarized $CD4^+$ T cells that express a differentiated memory T cell phenotype ([11-13]) and an oligoclonal T cell receptor (TCR) repertoire ([14, 15]). Importantly, the vast majority of Be-specific $CD4^+$ T cells recognize antigen in an HLA-DP-restricted manner ([16, 17]), and the HLA-DP molecules that mediate Be presentation match those implicated in disease susceptibility. These findings confirm that the mechanism of HLA contribution to disease susceptibility is based on the ability of those molecules to bind and present Be to pathogenic $CD4^+$ T cells ([16, 17]).

We recently developed an HLA-DP2 transgenic (Tg) murine model of Be-induced disease ([18]). Intratracheal exposure of these mice to Be oxide (BeO) induced mononuclear cell infiltrates in the lung and a Be-specific adaptive immune response in lung and spleen that was CD4-dependent and HLA-DP2-restricted. Using Be-loaded HLA-DP2 tetramers expressing either mimotope 2 or plexin A4 peptides ([19]), we identified a population of lung $CD4^+$ T cells in HLA-DP2 Tg mice that recognized the same TCR ligands as $CD4^+$ T cells derived from the bronchoalveolar lavage (BAL) of CBD patients. Thus, this murine model replicates the major features of the human disease and proves that expression of a single MHC class II (MHCII) molecule in a previously resistant mouse drives disease development upon environmental exposure to Be.

Here, we determined the TCR gene sequences expressed by Be-responsive $CD4^+$ T cells derived from the lungs of BeO-exposed HLA-DP2 Tg mice and investigated the spectrum of peptides that permit Be recognition by a subset of these TCRs. The TCR repertoire of these Be-responsive clones was dominated by expression of Vβ6 TCRs that were composed of identical or related complementarity determining region 3 (CDR3) sequences. We utilized a positional scanning peptide library ([19-22]) to screen a Vα4/Vβ6-expressing T cell transfectoma to determine if the peptides required to complete the αβTCR ligand possessed similar Be-coordinating amino acid residues as was previously observed for human Be-specific TCRs ([19]). As opposed to the identification of Be-dependent mimotopes ([19]), we identified mimotopes that stimulated the Be-specific T cell transfectomas in the absence of Be. These Be-independent mimotopes expressed arginine (R) and tryptophan (W) residues at the p5 and p7 positions of the peptide, respectively. We speculate that these distinct amino acids near the Be-binding site induce similar changes in charge and conformation to the HLA-DP2-peptide complex as those induced by the addition of the $Be^{2+}$ cation.

## RESULTS

### Expansion of Vβ6$^+$ CD4$^+$ T cells in the lung and BAL of BeO-exposed HLA-DP2 transgenic mice

To characterize the TCR repertoire of CD4$^+$ T cells present in the lung and spleen of HLA-DP2 Tg FVB/N mice, we pooled lung and spleen cells from 10 mice and determined the percentage of CD4$^+$ T cells expressing particular TCR Vβ regions using immunofluorescence staining (Figure 1). Because the FVB/N strain is characterized by a large genomic deletion in the *TCRB* gene locus ([23]), we focused on the limited set of expressed Vβs shown in Figure 1A. We noted an increased percentage of CD4$^+$ T cells expressing Vβ6 in the BAL and lung of BeO-exposed mice (Figure 1A and B). For example, compared to 11.1% of CD4$^+$ T cells in the lung of unexposed mice, 13.4% and 16.8% of lung and BAL CD4$^+$ T cells, respectively, expressed Vβ6 (Figure 1B). In addition, when gating on blasting (large forward scatter) T cells compared to a small lymphocyte gate (Figure 1C), the frequency of CD4$^+$ T cells expressing Vβ6 increased from 13.7% to 22.5% of BAL cells from 20 BeO-exposed HLA-DP2 Tg mice (Figure 1C and D). This distribution between blasting and small lymphocytes contrasted to other TCR Vβ subsets that either decreased in frequency or remained unchanged (Figure 1C and D). Collectively, these findings suggested that Vβ6$^+$ CD4$^+$ T cells are expanded in the lung and BAL after BeO exposure and may contain Be-responsive T cells.

### TCR gene expression of Be-specific T cell hybridomas derived from the lungs of BeO-exposed HLA-DP2 Tg mice

We have previously shown that the Be-specific adaptive immune response in BeO-exposed HLA-DP2 Tg mice is CD4$^+$ T cell-dependent ([18]). To characterize this Be-specific T cell population, lungs from 10 BeO-exposed HLA-DP2 Tg mice were harvested, and the pooled cells were stimulated in vitro with 10 μM $BeSO_4$. Blasting T cells were purified and expanded in IL-2 prior to fusing with TCR α$^-$/β$^-$ BW5147 thymoma cells. Of 90 T cell hybridomas screened for Be specificity, 29 were Be-responsive and secreted IL-2 after $BeSO_4$ exposure using an HLA-DP2-expressing murine fibroblast cell line as antigen-presenting cells (data not shown).

To determine *TCR* gene usage for each of the hybridomas, panels of *TCRAV* and *TCRBV* primers were used with TCR constant region primers to screen hybridoma cDNA by PCR. As shown in Figure 2A, *TCRAV4* and *TCRBV6* were the most commonly utilized V gene segments, being expressed in 45% and 55% of the Be-responsive hybridomas, respectively. *TCRAV* and *TCRBV* gene segment usage and CDR3 amino acid sequences of all of the Be-responsive T cell hybridomas are displayed in Figure 2B. Among the TCR Vβ6-expressing hybridomas, a CDR3β motif was evident in a subset of 5 hybridomas, utilizing different nucleotides to encode identical or nearly identical amino acid sequences with conserved CDR3 length and *TCRBJ* gene usage (Figure 3). Since some of the Vβ6-expressing hybridomas expressed multiple TCR α-chains (Figure 2B) and considering the genetic instability of the hybrids, we generated immortalized T cell transfectomas for each of the TCRs shown in Figure 3. For transfectoma LB9-18, the accompanying α-chain that conferred Be specificity was *TCRAV4S2* while the correct α-chain for LB10-17 was

*TCRAV1S1* (Figure S1). Similar to Be-specific TCRs derived from the lungs of CBD patients ([24], [25]), the oligoclonal Vβ6 chains were paired with different α-chains (Figure 3). Using these transfectomas in T cell stimulation assays, their ability to respond to $BeSO_4$ in vitro was equivalent to that of a Be-specific TCR (AV22) derived from the lungs of a CBD patient (Figure 4A).

We have previously shown that TCR recognition of the HLA-DP2-peptide/Be complex by human $CD4^+$ T cells requires glutamic acid (E) residues at positions 26, 68 and 69 of the HLA-DP2 β-chain ([26], [27]). For the human TCR AV22 and five murine T cell transfectomas, amino acid substitutions at these positions of the HLA-DP2-peptide/Be complex abrogated Be-induced IL-2 secretion (Figure 4B). Thus, these Be-specific TCRs derived from BeO-exposed HLA-DP2 Tg mice recognize the HLA-DP2-peptide/Be complex in a similar manner as TCRs derived from humans with CBD. The only difference was that AV22 had a partial reduction in IL-2 secretion with the EA68 HLA-DP2 β-chain variant while this mutation abolished the response of the murine TCRs (Figure 4B).

## TCR gene expression of Be-specific T cell hybridomas that recognize the HLA-DP2-PLXNA4/Be complex

We previously demonstrated that a subset of lung $CD4^+$ T cells from BeO-exposed mice recognized Be-loaded HLA-DP2 tetramers with either mimotope 2 or plexin A4 peptide in the peptide-binding groove ([18], [19]), the same TCR ligands found in CBD patients. Interestingly, all of the TCRs expressed on the Be-specific hybridomas in the current study, with the exception of LBM10-13, failed to bind either of these tetramers (data not shown). Using a T cell transfectoma expressing the AV22 TCR as a positive control for tetramer co-staining, Figure 5 shows that LBM10-13 bound to the HLA-DP2-plexinA4/Be tetramer but not to a Be-loaded HLA-DP2 tetramer expressing the highly related peptide, mimotope 2. The amino acid sequence of the plexin A4 epitope is FVDDLFETIF while that of mimotope 2 is FWIDLFELIG ([19]). Conversely, LB11-3 did not bind to either Be-loaded HLA-DP2-peptide tetramer. Thus, only one of the 29 Be-responsive T cell hybridomas derived from the lung of BeO-exposed HLA-DP2 Tg mice was specific for HLA-DP2-plexinA4/Be complex.

To identify additional $CD4^+$ T cells specific for this αβTCR ligand, lung cells from BeO-exposed HLA-DP2 Tg mice were stained with the HLA-DP2-PLXNA4/Be tetramer, and positively-staining cells were sorted for direct TCR sequencing. As shown in Figure 6A, we identified αβTCR pairs for three $CD4^+$ T cells. Interestingly, two of the three were highly-related to LBM10-13 that was identified in our initial screen, and both of these $V\beta16^+$ TCRs (scG-1 and scE-1) utilized *TCRAV4S9* with differing n and *AJ* regions (Figure 6A). To confirm antigen specificity, we expressed these TCRs on an $\alpha^-\beta^-$ immortalized cell line ([24]). Each of the TCRs was confirmed to be Be-specific and recognized the HLA-DP2-plexinA4/Be complex as demonstrated by tetramer staining (Figure 6B) and IL-2 secretion (Figure 9C). Similar to LBM10-13, none of these transfectomas bound the HLA-DP2-mimotope-2/Be tetramer (data not shown). Finally, the Be-specific TCR (scC-6) that stained with the highest affinity (highest MFI) also responded to the addition of PLXNA4/Be with greatest IL-2 secretion (i.e., lowest $EC_{50}$ value, defined as the peptide concentration inducing a half-maximal IL-2 response) (Figure 6B and C).

### Identification of TCR ligands using a decapeptide positional scanning library

Since the specific peptides required for T cell recognition of Be remained unknown for the vast majority of murine Be-specific TCRs, we utilized an unbiased decapeptide positional scanning library to systematically assess all peptides of a given length in a standard T cell activation assay ([19]). We focused on LB9-18 as a representative of the set of Be-specific Vβ6$^+$ T cell transfectomas expressing related oligoclonal TCRs (Figure 3). A surprisingly limited number of mixtures with particular amino acids fixed at certain positions of the peptide stimulated the LB9-18 TCR above background (Figure 7A). Specifically, the peptide mixtures that induced >20 pg/ml IL-2 secretion in the presence of $BeSO_4$ contained a glycine (G) at the p2 position, methionine (M) at p3, serine (S) at p4, arginine (R) and leucine (L) at p5, leucine (L) at p6, tryptophan (W) at p7, and tyrosine (Y) at p8 (Figure 7A). No definitive selection of amino acids was seen at the p1, p9 and p10 positions, although a possible preference for nonpolar amino acids (isoleucine (I) and valine (V)) was observed at p9.

Based on the preferences of the LB9-18 TCR for particular amino acids at each position of the peptide (Figure 7B), we synthesized a set of 14 mimotopes, also choosing to include mimotopes with a phenylalanine (F) at p1 since this amino acid is a preferred anchor residue for HLA-DP2 at this position ([19, 28]) (Figure 8A). These peptides were tested for their ability to stimulate the Be-specific T cell transfectomas. In Figure 8A, mimotopes were ranked based on IL-2 secretion by transfectoma LB9-18 with mimotopes 6, 5, 13, 7, 9 and 1 stimulating T cell activation and IL-2 secretion. However, only mimotopes 5, 6 and 13 induced IL-2 secretion at the lowest peptide concentration tested (0.5 μg/ml; Figure 8A). Interestingly, these mimotopes were Be-independent since they stimulated IL-2 secretion by the T cell transfectomas in the absence of $BeSO_4$ (LB9-18 shown in Figure 8B). Since mimotopes 5 and 6 only differed at the p1 position (T versus F), we focused on mimotope 6. T cell transfectoma LBM10-10 responded to mimotope 6 in a similar manner to LB9-18 with $EC_{50}$ values of 3.7 ± 0.2 and 6.8 ± 0.6 μM, respectively (Figure 8C). Conversely, LB10-17 responded less well (dose response curve shifted to the right; $EC_{50}$ = 26 ± 8.0 μM) (Figure 8C), and LBM11-8 and LBM12-1 did not respond at all (data not shown).

To determine the critical amino acids for either mimicking Be or interacting with the TCR, alanine (A) substitutions of mimotope 6 at positions p2, p3, p4, p5, p7 and p8 were synthesized and tested in the absence of Be. We chose not to alter p1 and p6 since these are known anchor residues ([19, 28]) and we could directly compare mimotope 6 and 5 (T versus F at p1). In addition, since no obvious amino acid selection was seen at p9 and p10 and we have previously shown that Be-specific TCRs do no contact these positions ([19, 29]), we did not further investigate p9 and p10. Using T cell transfectoma LB9-18, an F to T substitution at p1 of the peptide shifted the dose-response curve to the right, resulting in an 11-fold increase in the $EC_{50}$ value (Figure 9, upper panel). Alanines at the p3, p5 or p7 positions abrogated T cell recognition of the HLA-DP2-peptide/Be complex while A at p2, p4 or p8 had minimal effects on activation of the LB9-18 transfectoma (Figure 9, upper panel). LB9-18 and LB10-10 had a similar response to the alanine variants (Figure 9, middle panel). Conversely, LB10-17 had a 14-fold increase in $EC_{50}$ values for mimotope 6 and the variants and did not recognize the mimotope 6 A4 variant (Figure 9, lower panel).

Compared to Figure 4B where glutamic acids at position 26, 68 and 69 of the HLA-DP2 β-chain were required for Be-induced T cell activation of LB9-18 and LBM10-10, the addition of the Be-independent mimotope 6 eliminated the requirement for an E at position 26 (Figure S2). In addition, the presence of the isomorphic Q at this position enhanced IL-2 secretion by the transfectomas as compared to an A. Importantly, an E at positions 68 and 69 remained required even in the presence of mimotope 6 (Figure S2).

## DISCUSSION

CBD results from Be exposure in the workplace and the subsequent development of an adaptive immune response to the metal ([30]). Our previous studies have characterized the TCR repertoire ([14], [15]) and binding topology ([24], [25]) of Be-specific $CD4^+$ T cells derived from the blood and BAL of humans with CBD. In addition, recent analyses of the structure and function of HLA-DP2 in the context of CBD have shown that glutamic acid residues at positions 26, 68 and 69 of the HLA-DP2 β-chain are required for successful Be presentation to T cells ([27]), and the function of these amino acids is to capture and coordinate the $Be^{2+}$ cation ([29]). Although Be does not directly interact with the TCR, the addition of the $Be^{2+}$ cation induces both charge and conformational changes to the HLA-DP2-peptide complex that are subsequently recognized as a neoantigen ([29]). Here, we characterized the TCR repertoire of Be-responsive $CD4^+$ T cells in an HLA-DP2 Tg murine model of CBD ([18]) and identified $CD4^+$ T cells specific for the HLA-DP2-PLXNA4/Be complex. In addition, we identified Be-independent mimotopes for a set of highly related Vβ6-expressing $CD4^+$ T cells derived from the lungs of BeO-exposed HLA-DP2 Tg mice. Collectively, our findings expand our understanding of the interplay between Be and HLA-DP2-bound peptide in the generation of Be-induced hypersensitivity.

The ability of murine T cells to fuse with an immortal thymoma line enabled the characterization of TCRs derived from 29 Be-specific T cells, a quantity that far exceeds the total number of Be-specific T cell clones derived from CBD patients. Using an unbiased combinatorial peptide library approach, we identified mimotopes that stimulated Be-specific $V\beta6^+$ $CD4^+$ T cell transfectomas in the absence of Be. In contrast to previously identified Be-dependent mimotopes that possessed negatively-charged aspartic and glutamic acid residues at the p4 and p7 positions of the peptide ([19]), these mimotopes were composed of a positively-charged R at p5 and a bulky W at p7. Despite the differences, similar features included the preference for F at p1 and the absence of any significant selection for particular amino acids at the carboxy end of the peptide. A F at p1 has been shown by our group ([19]) and others ([28]) to be the preferred anchoring amino acid in the P1 pocket of HLA-DP2 while the lack of selection at the peptide carboxy end is likely due to the focus of the TCR on the center of the HLA-DP2-peptide complex ([29]).

The recently published structure of the HLA-DP2-mimotope 2/Be complex showed that binding of the $Be^{2+}$ cation reduced the electrostatic surface potential and changed the surface topology of the HLA-DP2-peptide complex where the AV22 TCR Vβ CDR3 interacts ([29]). Both of these changes must contribute to generation of the AV22 TCR ligand since this TCR is not stimulated by mimotope 2 without Be. In the absence of an HLA-DP2-mimotope 6 structure and insight into the actual Be-dependent epitope for the LB9-18 TCR,

we can only speculate on how this Be-independent mimotope might imitate the Be-specific TCR ligand. For example, the positively-charged R at the p5 position of the peptide may substitute for $Be^{2+}$ and reduce the electrostatic surface potential of the complex by partially neutralizing the solvent-exposed glutamic acids on HLA-DP2. In addition, the long side chain of R together with the bulky, hydrophobic W at p7 may create a conformation that mimics the conformation induced by the addition of $Be^{2+}$ and $Na^{+}$ to the MHCII-endogenous peptide complex ([29]). Of note, mutating E at positions 26, 68 and 69 of the HLA-DP2 β-chain abrogates Be-specific activation and IL-2 secretion of T cell clones and transfectomas ([17, 26, 29]). However, in the presence of Be-independent mimotope 6, fibroblasts expressing a variant HLA-DP2 molecule containing an isomorphic Q substitution at position 26 of the HLA-DP2 β-chain induced equivalent IL-2 secretion by the Be-specific T cell transfectoma, LB9-18, compared to fibroblasts expressing native HLA-DP2. Thus, our findings raise the possibility that the amino acid composition of the Be-independent mimotopes mimics the charge and structural changes induced by the addition of $Be^{2+}$ and $Na^{+}$ to the HLA-DP2-peptide complex.

Metal-independent mimotopes have been identified in other metal-induced hypersensitivities. For example, in subjects with nickel (Ni)-induced hypersensitivity, Ni-independent mimotopes were identified that replaced both the self-peptide and the $Ni^{2+}$ ion bound to HLA-DR52c ([31]). These mimotopes share a lysine (K) at the p7 position of the peptide. Structural analysis of a Ni-specific TCR interacting with HLA-DR52c-peptide complex showed that the interface was dominated by TCR Vβ CDR3 interacting with the exposed p7 K ([31]). These findings suggest that the $Ni^{2+}$ cation directly contributes to the TCR interaction, which would contrast with the indirect effects of the $Be^{2+}$ cation in altering both conformation and charge of HLA-DP2. Thus, the $Ni^{2+}$ and $Be^{2+}$ cations may generate an adaptive immune response and metal-induced hypersensitivity via different mechanisms, with $Ni^{2+}$ acting as a hapten and directly participating in TCR engagement while $Be^{2+}$ indirectly induces a post-translational alteration in an endogenous HLA-DP2-peptide complex. Collectively, these studies highlight the complexity of TCR recognition of metal-containing ligands.

When T cells derived from the site of pathology express the same Vβ and share a CDR3β motif, such as the $V\beta6^{+}$ Be-specific TCRs investigated in the current study, it is usually inferred that these TCRs respond to the same antigen. Thus, although mimotope 6 was identified through an unbiased screen using the Be-specific T cell transfectoma LB9-18, several of the other T cell transfectomas were stimulated by this peptide. T cell transfectomas LBM10-10 and LB10-17 responded to mimotope 6 presented by HLA-DP2 with varying affinities while LBM11-8 and LBM12-1 did not recognize it at all. LB9-18 and LBM10-10 recognized this MHCII-peptide complex with lower $EC_{50}$ values compared to LB10-17. Thus, since the TCR β-chains of these three TCRs are identical, the differences in TCR affinity are due to the different α-chains expressed by these cells. In this regard, while both LB9-18 and LBM10-10 express Vα4 and Jα22, LB10-17 expresses Vα1 and Jα45 and has a 5-10-fold higher $EC_{50}$ than the other two Be-specific TCRs. In addition, the inability of LBM11-8 and LBM12-1 to respond to mimotope 6 likely stems from a combination of an R at position 95 of the TCR β-chain and expression of Vα1. Thus, the response to mimotope

6 clearly relates to similarities of the recognizing TCRs (e.g., LB9-18 ≥ LBM10-10 > LB10-17 >> LBM11-8/LBM12-1).

In conjunction with characterizing the overall T cell response to Be, we further analyzed murine-derived $CD4^+$ T cells specific to the HLA-DP2-PLXNA4/Be complex, a T cell specificity found in all HLA-$DP2^+$ CBD subjects ([19]). In the initial analysis, only one of the 29 Be-specific hybridomas stained with the Be-loaded HLA-DP2-PLXNA4 tetramer. Thus, we confirmed our previous finding that these T cells are present in BeO-exposed HLA-DP2 Tg mice ([18]), although they do not represent a major specificity. Further analysis of single-cell sorted tetramer-binding T cells enabled the identification of the TCR genes expressed by 3 additional T cell clones. Two of these clones expressed homologous $V\beta16^+/V\alpha4^+$ TCRs that closely matched the sequence of the LBM10-13 TCR while the third clone expressed a completely unrelated $V\beta6^+$ TCR. Similar to LBM10-13, none of these TCRs recognized the HLA-DP2-mimotope 2/Be tetramer. Thus, tetramer co-staining patterns at the clonal level verified our previous findings of bulk BAL T cells derived from CBD patients ([19]). In essence, subsets of T cells exist that either co-stain with mimotope 2 and plexin A4 tetramers or only bind to the tetramer presenting the endogenous antigen (plexin A4/Be). These differences likely reflect dissimilarities in TCR sequence among the antigen-specific population and are an important consideration when using a mimotope selected by a single TCR.

In the lungs of CBD patients, we previously identified Be-specific TCRs that were HLA-DP2-restricted, expressed nearly identical TCR Vβ5.1 chains while coupled with different TCR α-chains ([24]) and comprised a public TCR repertoire ([25]). Results in BeO-exposed HLA-DP2 Tg mice mirror what has been observed in human disease (i.e., identification of clonally expanded $V\beta6^+$ Be-specific TCRs expressing identical or nearly identical β-chains coupled with differing TCR α-chains). These findings suggest that the Be-specific TCRs derived from both HLA-DP2-expressing mice and humans recognize the HLA-DP2-peptide/Be complex in a similar manner, with the majority of interactions contributed by TCR Vβ residues and the HLA-DP2 β1-chain ([29]). These findings provide further validation for the use of the HLA-DP2 Tg murine model to study the initiation of a Be-specific adaptive immune response.

The identification of Be-independent mimotopes that mimic a Be-modified HLA-DP2-peptide complex raises the possibility that such peptides exist in vivo and can be involved in the maintenance of the Be-specific T cell response. We found, however, that $CD4^+$ T cells derived from the lungs of BeO-exposed HLA-DP2 Tg mice and Be-specific $CD4^+$ T cell lines derived from CBD patients do not secrete IFN-γ or IL-2 in response to the Be-independent mimotope 6 (data not shown). In addition, preliminary experiments studying adoptively-transferred $V\beta6^+$ $CD4^+$ T cells derived from the lungs of BeO-exposed HLA-DP2 Tg mice showed that this cell population failed to preferentially home to or expand in recipient lungs compared to spleen in the absence of BeO exposure (data not shown). Collectively, these data suggest that T cells reactive to these Be-independent mimotopes do not exist in vivo. It is likely that the persistent inflammation seen in HLA-DP2-expressing mice and CBD patients is secondary to persistent antigen exposure since Be remains within lung granulomas for decades after the cessation of exposure ([32]).

In conclusion, the present work identifies Be-independent mimotopes for a set of oligoclonal TCRs derived from the lungs of BeO-exposed HLA-DP2 Tg mice. The utilization of highly-related TCR β-chains paired with different α-chains suggests that TCR interactions with the Be antigen are dominated by the TCR β-chain, regardless of species. Although the Be-independent mimotopes likely do not have in vivo relevance, they further our understanding of Be-induced alterations in the topology of the HLA-DP2-peptide complex. Future studies utilizing TCR Tg mice expressing HLA-DP2-plexin A4/Be or Vβ6 Be-specific TCRs will enable us to define mechanisms of disease pathogenesis. Thus, HLA-DP2 Tg mice provide a powerful tool for the dissection of the role of Be-specific $CD4^+$ T cells in the generation of Be-induced hypersensitivity.

## METHODS

### Exposure of mice to Be and preparation of lung cells

HLA-DP2 (*HLA-DPA1*0103* and -*DPB1*0201*) Tg mice on an FVB/N background were generated as previously described ([18], [33]). Mice were bred and maintained in the Biological Resource Center at the University of Colorado Denver in accordance with the National Institutes of Health guidelines for use of live animals. All experiments were conducted with the approval of the Institutional Animal Care and Use Committee of the University of Colorado Denver.

Six to eight week old HLA-DP2 Tg FVB/N mice were anesthetized with isoflurane, and 100 μg BeO (NIST, standard reference material 1877) was administered via oropharyngeal aspiration on days 0, 1, 2, 14, 15, 18 and 19 ([18]). Mice were sacrificed on day 21, and single cell suspensions of splenocytes were prepared ([18]). Harvested lungs were minced and digested in tissue culture medium containing 1 mg/ml collagenase (Sigma-Aldrich). After 30 minutes at 37°C, digested lung tissue was disrupted, and the lung cells were centrifuged. After lysis of erythrocytes, lung cells were filtered through a 70 μM cell strainer and resuspended in complete tumor media (CTM), consisting of MEM, 10% fetal bovine serum and 6% tumor cocktail as previously described ([34]). Collection of BAL cells was performed by three successive intratracheal instillations of 0.5 ml PBS.

### Generation of Be-specific T cell hybridomas

Be-specific T cell hybridomas were generated as previously described ([35]). In brief, lung cell suspensions from 10 mice were pooled and restimulated in vitro at $2 \times 10^6$/ml with 10 μM $BeSO_4$ in CTM. After four days in culture, T cell blasts were enriched by density gradient centrifugation (Histopaque, Sigma-Aldrich) and expanded in IL-2 for three days. T cell hybridomas were established by fusion of T cells to TCR $\alpha^-/\beta^-$ BW5147 thymoma cells using polyethylene glycol and cloned by limiting dilution under hypoxanthine, aminopterin, and thymidine (HAT) (Invitrogen) selection. T cell hybridoma clones were screened for Be specificity by measuring IL-2 production by ELISA (eBioscience) after stimulation with 200 μM $BeSO_4$ presented by an HLA-DP2-transfected murine fibroblast, designated DP8302.

### Determination of TCRA and TCRB gene usage

To determine *TCRB* gene usage, total RNA was isolated using a Qiagen RNeasy kit (Qiagen), and cDNA was prepared as previously described ([14]). *TCRB* gene fragments were PCR-amplified using a 3′ *TCRBC* primer and a panel of BV primers (n = 13) to screen for *TCRBV* gene usage of each of the hybridomas. An identical PCR screening methodology was employed to determine *TCRAV* gene segment usage, using a 3′ *TCRAC* primer and panel of AV primers (n = 22). Upon determination of specific *BV* and *AV* gene segment usage, larger scale PCR reactions were completed, and products were purified using a DNA binding membrane spin column (Qiagen), and sequenced (Applied Biosystems).

### Transfectomas expressing particular murine Be-specific TCRs

Because T cell hybridomas created by fusing murine T cells with BW5147 cells are tetraploid and genetically unstable, TCRs expressed by select Be-specific hybridomas were cloned into expression vectors and stably transfected into the mouse hybridoma cell line 54ζ, which expresses human CD4 ([19, 24, 25, 36]), as described in the Online Supplement.

### Decapeptide positional scanning library and peptide synthesis

The decapeptide library used for this study (designated TPIMS 2040) is a synthetic N-acetylated, C-terminal amidated, L-amino acid combinatorial peptide library organized in a positional scanning format. This library consists of 200 mixtures prepared in an OX9 format where O represents a specific amino acid at a defined position and X represents an equimolar mixture of all natural amino acids (except cysteine) in each of the remaining 9 positions. Each OX9 mixture consists of $3.2 \times 10^{11}$ different decapeptides, and the total number of peptides in the library is $6.4 \times 10^{12}$ ([22, 37]). T cell transfectoma response to HLA-DP2-expressing fibroblasts presenting peptide mixtures in the presence of Be was assessed by IL-2 secretion. The amount of IL-2 secreted in wells not containing mixtures was subtracted from IL-2 values obtained from wells that included mixtures to yield net IL-2 (pg/ml).

Individual candidate peptides (mimotopes), selected based on analysis of positional scanning results, were synthesized using the PEPScreen 96-well array (Sigma). Peptides chosen for further studies were synthesized on a larger scale and tested at 95% purity (CPC Scientific). All peptides were first dissolved in DMSO at high concentration prior to making a working stock in PBS.

### HLA-DP2-PLXNA4/Be tetramer staining and cell sorting

Preparation of soluble, Be-loaded HLA-DP2-covalent plexin A4 peptide (PLXNA4) tetramers was performed as previously described ([19]). For sorting of HLA-DP2 tetramer-binding $CD4^+$ T cells, lung cells ($5\text{-}10 \times 10^6$ cells per mouse) from BeO-exposed HLA-DP2 Tg FVB/N mice were incubated in 25 μl of medium containing 5 μM sodium azide, an excess of FcR-specific blocking mAb and the PE-labeled HLA-DP2-PLXNA4/Be tetramer (20 μg/ml). After 2 hrs at 37°C, fluorescently-conjugated mAbs to murine CD3 (PE-Cy7), CD4 (AF700), CD11c (APC-eFluor 780), B220 (eFluor 450), F4/80 (eFluor 450), CD8 (eFluor 450) and CD44 (PerCP-Cy5.5) were added, and cells were incubated at 4°C an additional 30 min. After washing, cells were analyzed on a FACSAria flow cytometer (BD

Immunocytometry Systems). Cells staining with mAbs directed against B220, F4/80 and CD8 and CD11c were included in a dump gate and excluded from analysis. Using forward and side scatter patterns, dump-negative, $CD3^+CD4^+$ T cells were selected and sorted based on tetramer staining and high CD44 expression.

### Cloning of PLXNA4/Be-specific TCRs from $CD4^+$ T cells isolated by single cell sorting

A single cell suspension was prepared from the lungs of BeO-exposed HLA-DP2 Tg mice as described previously ([18]). Cells were stained with mAbs directed against CD4 (AF700), CD3 (PE-Cy7), CD8 (eFluor 450), B220 (eFluor 450), F4/80 (eFluor 450), CD44 (PerCP-Cy5.5), and PE-labeled HLA-DP2-PLXNA4/Be tetramer ([19]). $Tetramer^+CD3^+CD4^+CD44^+$ T cells were single cell sorted into reverse transcription buffer in a 96-well plate using a FACSAria flow cytometer. *TCRAV* and *TCRBV* gene expression was determined using 5′ RACE and a nested PCR method as previously described ([25], [38]) and as detailed in the Online Supplement.

## Supplementary Material

Refer to Web version on PubMed Central for supplementary material.

## Acknowledgements

This work is supported by the following NIH grants: HL111760, HL62410 and ES11810 (to APF). The authors thank Marc Giulianotti for synthesis of the decapeptide positional scanning library TPIMS 2040 and Amy McKee for technical assistance.

## References

1. Richeldi L, Sorrentino R, Saltini C. HLA-DPB1 glutamate 69: a genetic marker of beryllium disease. Science. 1993; 262:242–244. [PubMed: 8105536]
2. Richeldi L, et al. Interaction of genetic and exposure factors in the prevalence of berylliosis. Am J Ind Med. 1997; 32:337–340. [PubMed: 9258386]
3. Wang Z, et al. Differential susceptibilities to chronic beryllium disease contributed by different Glu69 HLA-DPB1 and -DPA1 alleles. J Immunol. 1999; 163:1647–1653. [PubMed: 10415070]
4. Rossman MD, et al. Human leukocyte antigen Class II amino acid epitopes: susceptibility and progression markers for beryllium hypersensitivity. Am J Respir Crit Care Med. 2002; 165:788–794. [PubMed: 11897645]
5. Maier LA, et al. Influence of MHC class II in susceptibility to beryllium sensitization and chronic beryllium disease. J Immunol. 2003; 171:6910–6918. [PubMed: 14662898]
6. McCanlies EC, Ensey JS, Schuler CR, Kreiss K, Weston A. The association between HLA-DPB1Glu69 and chronic beryllium disease and beryllium sensitization. Am J Ind Med. 2004; 46:95–103. [PubMed: 15273960]
7. Van Dyke MV, et al. Risk of chronic beryllium disease by HLA-DPB1 E69 genotype and beryllium exposure in nuclear workers. Am J Respir Crit Care Med. 2011; 183:1680–1688. [PubMed: 21471109]
8. Kreiss K, Mroz MM, Newman LS, Martyny J, Zhen B. Machining risk of beryllium disease and sensitization with median exposures below 2 $mg/m^3$. Am J Ind Med. 1996; 30:16–25. [PubMed: 8837677]
9. Kreiss K, Mroz MM, Zhen B, Martyny JW, Newman LS. Epidemiology of beryllium sensitization and disease in nuclear workers. Am Rev Respir Dis. 1993; 148:985–991. [PubMed: 8214955]

10. Kreiss K, Wasserman S, Mroz MM, Newman LS. Beryllium disease screening in the ceramics industry: blood test performance and exposure-disease relations. J Occup Med. 1993; 35:267–274. [PubMed: 8455096]
11. Fontenot AP, Canavera SJ, Gharavi L, Newman LS, Kotzin BL. Target organ localization of memory $CD4^+$ T cells in patients with chronic beryllium disease. J Clin Invest. 2002; 110:1473–1482. [PubMed: 12438445]
12. Fontenot AP, et al. CD28 costimulation independence of target organ versus circulating memory antigen-specific $CD4^+$ T cells. J Clin Invest. 2003; 112:776–784. [PubMed: 12952926]
13. Fontenot AP, et al. Frequency of beryllium-specific, central memory CD4+ T cells in blood determines proliferative response. J Clin Invest. 2005; 115:2886–2893. [PubMed: 16151531]
14. Fontenot AP, Falta MT, Freed BM, Newman LS, Kotzin BL. Identification of pathogenic T cells in patients with beryllium-induced lung disease. J Immunol. 1999; 163:1019–1026. [PubMed: 10395700]
15. Fontenot AP, Kotzin BL, Comment CE, Newman LS. Expansions of T-cell subsets expressing particular T cell receptor variable regions in chronic beryllium disease. Am J Respir Cell Mol Biol. 1998; 18:581–589. [PubMed: 9533947]
16. Fontenot AP, Torres M, Marshall WH, Newman LS, Kotzin BL. Beryllium presentation to $CD4^+$ T cells underlies disease susceptibility HLA-DP alleles in chronic beryllium disease. Proc Natl Acad Sci U S A. 2000; 97:12717–12722. [PubMed: 11050177]
17. Lombardi G, et al. HLA-DP allele-specific T cell responses to beryllium account for DP-associated susceptibility to chronic beryllium disease. J Immunol. 2001; 166:3549–3555. [PubMed: 11207315]
18. Mack DG, et al. Regulatory T cells modulate granulomatous inflammation in an HLA-DP2 transgenic murine model of beryllium-induced disease. Proc Natl Acad Sci U S A. 2014; 111:8553–8558. [PubMed: 24912188]
19. Falta MT, et al. Identification of beryllium-dependent peptides recognized by $CD4^+$ T cells in chronic beryllium disease. J Exp Med. 2013; 210:1403–1418. [PubMed: 23797096]
20. Hemmer B, et al. The use of soluble synthetic peptide combinatorial libraries to determine antigen recognition of T cells. J Pept Res. 1998; 52:338–345. [PubMed: 9894839]
21. Pinilla C, Appel JR, Blanc P, Houghten RA. Rapid identification of high affinity peptide ligands using positional scanning synthetic peptide combinatorial libraries. Biotechniques. 1992; 13:901–905. [PubMed: 1476743]
22. Pinilla C, Appel JR, Houghten RA. Investigation of antigen-antibody interactions using a soluble, non-support-bound synthetic decapeptide library composed of four trillion ($4 \times 10^{12}$) sequences. Biochem J. 1994; 301:847–853. [PubMed: 7519851]
23. Osman GE, et al. FVB/N (H2(q)) mouse is resistant to arthritis induction and exhibits a genomic deletion of T-cell receptor V beta gene segments. Immunogenetics. 1999; 49:851–859. [PubMed: 10436178]
24. Bowerman NA, Falta MT, Mack DG, Kappler JW, Fontenot AP. Mutagenesis of beryllium-specific TCRs suggests an unusual binding topology for antigen recognition. J Immunol. 2011; 187:3694–3703. [PubMed: 21873524]
25. Bowerman NA, et al. Identification of multiple public T cell receptor repertoires in chronic beryllium disease. J Immunol. 2014; 192:4571–4580. [PubMed: 24719461]
26. Bill JR, et al. Beryllium presentation to $CD4^+$ T cells is dependent on a single amino acid residue of the MHC class II b-chain. J Immunol. 2005; 175:7029–7037. [PubMed: 16272364]
27. Dai S, et al. Crystal structure of HLA-DP2: Implications for chronic beryllium disease. Proc Natl Acad Sci U S A. 2010; 107:7425–7430. [PubMed: 20356827]
28. Sidney J, et al. Five HLA-DP molecules frequently expressed in the worldwide human population share a common HLA supertypic binding specificity. J Immunol. 2010; 184:2492–2503. [PubMed: 20139279]
29. Clayton GM, et al. Structural basis of chronic beryllium disease: linking allergic hypersensitivity and autoimmunity. Cell. 2014; 158:132–142. [PubMed: 24995984]
30. Fontenot AP, Maier LA. Genetic susceptibility and immune-mediated destruction in beryllium-induced disease. Trends Immunol. 2005; 26:543–549. [PubMed: 16099719]

31. Yin L, Crawford F, Marrack P, Kappler JW, Dai S. T-cell receptor (TCR) interaction with peptides that mimic nickel offers insight into nickel contact allergy. Proc Natl Acad Sci U S A. 2012; 109:18517–18522. [PubMed: 23091041]

32. Sawyer RT, Abraham JL, Daniloff E, Newman LS. Secondary ion mass spectroscopy demonstrates retention of beryllium in chronic beryllium disease granulomas. J Occup Environ Med. 2005; 47:1218–1226. [PubMed: 16340702]

33. Tarantino-Hutchison LM, et al. Genetic determinants of sensitivity to beryllium in mice. J Immunotoxicol. 2009; 6:130–135. [PubMed: 19589099]

34. Kappler JW, Skidmore B, White J, Marrack P. Antigen-inducible, H-2-restricted, interleukin-2 producing T cell hybridomas: lack of independent antigen and H-2 recognition. J Exp Med. 1981; 153:1198. [PubMed: 6166712]

35. Ignatowicz L, Kappler J, Marrack P. The repertoire of T cells shaped by a single MHC/peptide ligand. Cell. 1996; 84:521–529. [PubMed: 8598039]

36. Boen E, Crownover AR, McIlhaney M, Korman AJ, Bill J. Identification of T cell ligands in a library of peptides covalently attached to HLA-DR4. J Immunol. 2000; 165:2040–2047. [PubMed: 10925287]

37. Hemmer B, et al. Identification of candidate T-cell epitopes and molecular mimics in chronic Lyme disease. Nat Med. 1999; 5:1375–1382. [PubMed: 10581079]

38. Ozawa T, Tajiri K, Kishi H, Muraguchi A. Comprehensive analysis of the functional TCR repertoire at the single-cell level. Biochemical and biophysical research communications. 2008; 367:820–825. [PubMed: 18191637]

39. Arden B, Clark SP, Kabelitz D, Mak TW. Mouse T-cell receptor variable gene segment families. Immunogenetics. 1995; 42:501–530. [PubMed: 8550093]

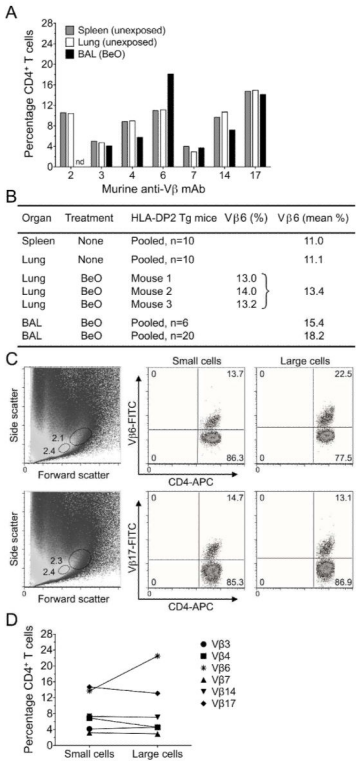


**Figure 1.**

TCR Vβ repertoire of CD4$^+$ T cells in HLA-DP2 Tg FVB/N mice. (A) Percentage of CD4$^+$ T cells expressing particular TCR Vβ-chains are shown for pooled lung and spleen cells (n = 10) from untreated HLA-DP2 Tg mice and pooled BAL cells (n = 20) isolated from HLA-DP2 Tg mice exposed to BeO. mAbs chosen were based on the known genomic deletion within the *TCRB* locus of FVB/N mice and the availability of anti-TCR Vβ reagents. The seven mAbs in the panel account for >60% of the total Vβ repertoire. nd: not determined (B) Summary of CD4$^+$ T cell expression of Vβ6 in different cell populations of untreated or BeO-exposed HLA-DP2 Tg mice. BAL cells from multiple treated mice were pooled in order to have enough cells to perform the analysis. (C) Representative density plots of CD4/Vβ6 (top plots) and CD4/Vβ17 (bottom plots) staining of BAL T cells obtained by pooling cells from 20 BeO-exposed HLA-DP2 Tg mice are shown. Forward by side scatter plots (left) were used to gate small and blasting lymphocyte populations and compare Vβ expression within each subset. In the CD4/Vβ plots, the number in the upper right quadrant indicates the percentage of CD4$^+$ T cells expressing the particular Vβ. (D) Summary of the frequency of CD4$^+$ T cells expressing particular Vβs in small and blasting (large) lymphocyte gates. Data show that Vβ6 is the only T cell population enriched in the blasting T cell population compared to small lymphocytes.

A

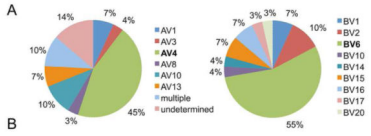


B

| Hyb | BV | Vβ | NDβN | Jβ | BJ | AV | Vα | N | Jα | AJ |
|---|---|---|---|---|---|---|---|---|---|---|
| LB12-17 | 1S1 | CASS | QLTDTS | YAEQFFG | 2S1 | 4S9 | CAL | SST | ASLGKLQFG | 24 |
| LB10-7 | 1S1 | CASS | QTGNF | YEQYFG | 2S7 | 4.nd | CA | P | NNAGAKLTFG | 39 |
| LB9-13 | 2S1 | CSAD | HLGG | YAEQFFG | 2S1 | 13S1 | CAA | SV | YNVLYFG | 21 |
| LB12-3 | 2S1 | CSAD | HRGG | AETLYFG | 2S3 | 13S1 | CAA | S | NYNVLYFG | 21 |
| LB12-4 | 2S1 | CTCS | AAGGAR | AETLYFG | 2S3 | 4S2 | CAL | GEG | DSGTYQRFG | 13 |
| LB11-3 | 3S1 | CASS | LGRA | NTLYFG | 1S3 | 4S9 | CAL | SL | NTGNYKYVFG | 40 |
| LB9-17 | 6S1 | CASS | LNA | NTEVFFG | 1S1 | ND | | | | |
| LB11-4 | 6S1 | CASS | RTNS | YNSPLYFA | 1S6 | 10S3 | CAM | E | NMGYKLTFG | 9 |
| LBM9-5 | 6S1 | CASS | RQGL | NSPLYFA | 1S6 | 10S3 | CAM | DR | DTNAYKVIFG | 30 |
| LB11-2 | 6S1 | CASS | STGGWD | AEQFFG | 2S1 | 4S11 | C | VL | GTGGYKVVFG | 12 |
| LB9-18 | 6S1 | CASS | ILGG | QNTLYFG | 2S4 | 4S2* | CAL | Q | SSGSWQLIFG | 22 |
| | | | | | | 13S1 | CAA | RR | NNYAQGLTFG | 26 |
| LB10-9 | 6S1 | CASS | ILGG | QNTLYFG | 2S4 | 4S2* | CAL | Q | SSGSWQLIFG | 22 |
| | | | | | | 13S1 | CAA | RR | NNYAQGLTFG | 26 |
| LBM10-10 | 6S1 | CASS | ILGG | QNTLYFG | 2S4 | 4S9 | CAL | S | SSGSWQLIFG | 22 |
| LB11-9 | 6S1 | CASS | ILGG | QNTLYFG | 2S4 | 4S9 | CAL | S | SSGSWQLIFG | 22 |
| LB10-17 | 6S1 | CASS | ILGG | QNTLYFG | 2S4 | 1S1* | CAV | T | TGGADRLTG | 45 |
| | | | | | | 10S6 | C | ARL | SNTDKVVFG | 34 |
| LBM12-1 | 6S1 | CAS | TRLGG | QNTLYFG | 2S4 | 1S3 | CAVS | P | SGSWQLIFG | 22 |
| LBM11-8 | 6S1 | CASS | RLGG | QDTQYFG | 2S5 | 1S3 | CAVS | | TGGADRLTFG | 45 |
| LBM11-1 | 6S1 | CASS | IRGGY | QDTQYFG | 2S5 | 3.nd | CAVS | P | MGYKLTFG | 9 |
| LBM9-1 | 6S1 | CAS | RGGG | DTQYFG | 2S5 | 10.nd | CAM | L | SSGSWQLIFG | 22 |
| LB9-5 | 6S1 | CAS | RQG | DTQYFG | 2S5 | 4S9 | CAL | SP | SGGSNAKLTFG | 42 |
| LB10-16 | 6S1 | CASS | WTGP | DTQYFG | 2S5 | ND | | | | |
| LBM9-18 | 14S1 | CAWS | PGTN | SGNTLYFG | 1S3 | ND | | | | |
| LB9-14 | 15S1 | CGAR | GTGS | SQNTLYFG | 2S4 | 4S11 | CVL | GERA | GNTRKLIFG | 37 |
| | | | | | | 4.nd | CAL | GA | YAQGLTFG | 26 |
| LB10-12 | 15S1 | CGAA | GTGGL | QDTQYFG | 2S5 | ND | | | | |
| LBM9-13 | 16S1 | CASS | LKGG | QNTLYFG | 2S4 | 4S9 | CAL | TS | NTGYQNFYF | 49 |
| LBM10-13 | 16S1 | CASS | LGGR | NTQYFG | 2S5 | 4S9 | CAL | SP | NTGYQNFYFG | 49 |
| LB11-8 | 17S1 | CASS | PRGG | YNSPLYFA | 1S6 | 3.nd | CAVS | AD | YGGSGNKLIFG | 32 |
| | | | | | | 20S1 | CAA | V | NSGGSNYKLTFG | 53 |
| LBM9-4 | 20.nd | CSS | RPRQGWD | TEVFFG | 1S1 | 4S2 | CAL | R | ATGGNNKLTFG | 56 |
| LBM10-21 | ND | | | | | 8S3/S9 | CALS | DGG | GSALGRLHFG | 18 |

**Figure 2.**

TCR gene expression of Be-specific T cell hybridomas. (A) Pie charts show the frequency of *TCRAV* (left) and *TCRBV* (right) gene segment usage of 29 Be-specific T cell hybridomas derived from the lungs of BeO-exposed HLA-DP2 transgenic mice. (B) Shown are *TCR* gene segment usage and junctional region amino acid sequences of Be-specific T cell hybridomas. Identified *TCRB* and *TCRA* V and J gene segments are indicated using the nomenclature of Arden et al. ([39]). In some instances, precise V gene segment usage (ND) or subfamily usage (nd) could not be assigned. Also presented are the deduced CDR3 amino acid sequences of the *TCRB* and *TCRA* genes beginning at the conserved cysteine (C) of the expressed V gene segment and ending at the conserved phenylalanine-glycine (FG) of the J gene segment. Two pairs of hybridomas (LB9-18/LB10-9 and LBM10-10/LB11-9) were duplicate clonal isolates sharing identical nucleotide sequences. In four instances, two functional *TCRA* genes were obtained for an individual hybridoma. The correct TCR α/β chain pair conferring Be specificity (denoted by an asterisk) was determined for three of these hybridomas by separately expressing the TCRs on recipient hybridoma cell lines and testing for Be-specificity by IL-2 ELISA.

| Clone | BV6S1 | | | | NBDN | | | | BJ2S4 | | | | | | | AV use |
|---|---|---|---|---|---|---|---|---|---|---|---|---|---|---|---|---|
| | 91 | | | | 95 | | | | 99 | | | | | | | |
| LB9-18 | C | A | S | S | I | L | G | G | Q | N | T | L | Y | F | G | AV4S2 |
| | TGT | GCC | AGC | AGT | ATA | CTG | GGA | GGG | CAA | AAC | ACC | TTG | TAC | TTT | GGT | |
| LBM10-10 | C | A | S | S | I | L | G | G | Q | N | T | L | Y | F | G | AV4S9 |
| | TGT | GCC | AGC | AGT | ATT | CTG | GGG | GGG | CAA | AAC | ACC | TTG | TAC | TTT | GGT | |
| LB10-17 | C | A | S | S | I | L | G | G | Q | N | T | L | Y | F | G | AV1S1 |
| | TGT | GCC | AGC | AGT | ATT | CTG | GGG | GGC | CAA | AAC | ACC | TTG | TAC | TTT | GGT | |
| LBM11-8 | C | A | S | S | R | L | G | G | Q | D | T | Q | Y | F | G | AV1S3 |
| | TGT | GCC | AGC | AGT | CGA | CTG | GGG | GGT | CAA | GAC | ACC | CAG | TAC | TTT | GGG | |
| LBM12-1 | C | A | S | T | R | L | G | G | Q | N | T | L | Y | F | G | AV1S3 |
| | TGT | GCC | AGC | ACC | CGA | CTG | GGG | GGC | CAA | AAC | ACC | TTG | TAC | TTT | GGT | |

**Figure 3.**

TCR CDR3β nucleotide and deduced amino acid sequences from a related set of Be-specific Vβ6.1$^{+}$ T cell hybridomas. Variations in nucleotide and deduced amino acid sequence compared to hybridoma LB9-18 are underlined. Note hybridoma LBM11-8 expresses *TCRBJ2S5*; the others in this set express *BJ2S4*. Also indicated is *TCRAV* gene use for each hybridoma. The cysteine (C) of the β-chain is designated as position 91 with the NβDN and the Jβ region beginning at positions 95 and 99, respectively.

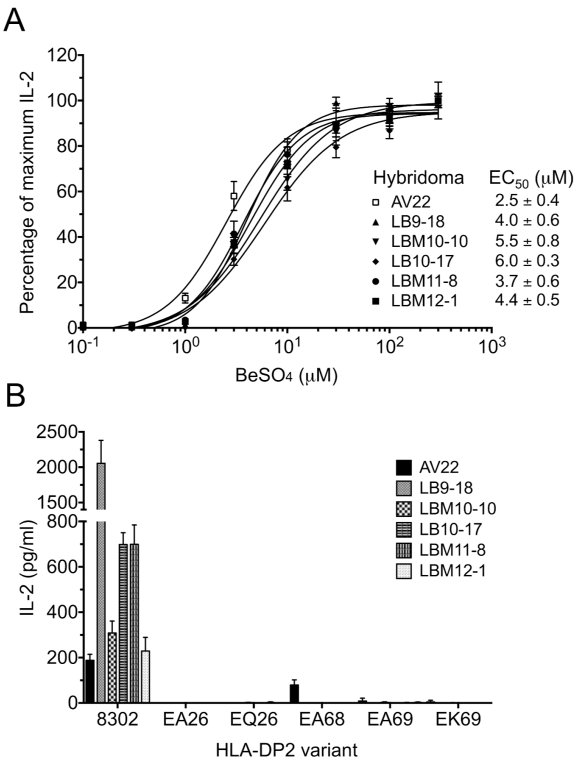


**Figure 4.**

T cell transfectoma response to Be. (A) Select T cell transfectomas were stimulated with an equal number of HLA-DP2-transfected fibroblasts (designated 8302) as antigen-presenting cells and various amounts of $BeSO_4$ (0.3 μM to 300 μM) in FBS-containing medium. IL-2 secretion (mean ± SEM pg/ml) was measured by ELISA after 22 hrs of culture, and data was plotted as the percentage of maximum IL-2 secretion against $BeSO_4$ concentration. Mean $EC_{50}$ values (concentration of $BeSO_4$ that results in a half-maximal T cell transfectoma response) (μM) for each transfectoma were determined by nonlinear regression of the activation curves using Prism software (GraphPad). The AV22 transfectoma, expressing a human $V\beta5.1^+/V\alpha22^+$ TCR derived from lung of a CBD patient ([24]) is shown for comparison. Dose-response curves are representative of three independent experiments done in triplicate. (B) Be-induced IL-2 secretion (pg/ml) by AV22 and the five murine $V\beta6^+$ T cell transfectomas in response to $BeSO_4$ presentation by fibroblasts expressing either wt HLA-DP2 or HLA-DP2 variants with alanine, glutamine or lysine substitutions at positions 26, 68, and 69 of the β-chain is shown.

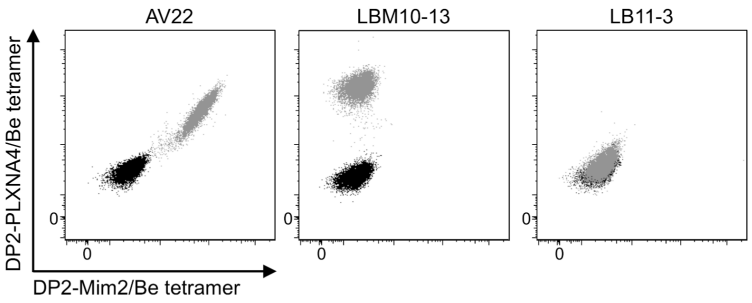


**Figure 5.**

HLA-DP2-peptide/Be tetramer staining of Be-responsive T cell transfectomas. Co-staining of three Be-specific transfectomas (AV22, LBM10-13, and LB11-3) with Be-saturated HLA-DP2-mimotope-2 (BV421-labeled) and HLA-DP2-PLXNA4 (PE-labeled) tetramers (shown in blue) compared to unstained cells (shown in red). Representative results from three independent experiments are shown.

A

| Clone | BV use | Vβ | NDβN | Jβ | BJ | AV use | Vα | N | Jα | AJ |
|---|---|---|---|---|---|---|---|---|---|---|
| LBM10-13 | BV16S1 | CASS | **LGGRN** | TQYFG | 2S5 | AV4S9 | CAL | **SP** | NTGYQNFYFG | 49 |
| scG-1 | BV16S1 | CASS | L**GGRN** | TQYFG | 2S5 | AV4S9 | CAL | **SDL** | GTYQRFG | 13 |
| scE-1 | BV16S1 | CASS | L**GGR**N | TLYFG | 2S4 | AV4S9 | CAL | **SDMG** | AQGLTFG | 26 |
| scC-6 | BV6S1 | CAS**S** | **RTGVR** | YAEQFFG | 2S1 | AV3 | CAV | **RY** | NRIFFG | 31 |

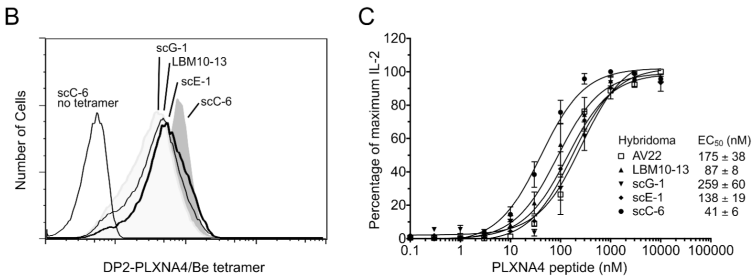


**Figure 6.**

Characterization of HLA-DP2-PLXNA4/Be-specific murine T cells. (A) Shown are TCR gene segment usage and junctional region amino acid sequences of $CD4^+$ T cells specific for the HLA-DP2-PLXNA4/Be complex. LBM10-13 was derived by fusing T cells from the lung of BeO-exposed HLA-DP2 Tg mice to $\alpha^-/\beta^-$ BW5147 thymoma cells to generate a TCR-expressing hybridoma. The other TCRs were identified by 5′ RACE and PCR from $CD4^+$ $CD44^+$ T cells that were individually sorted by flow cytometry for binding to the HLA-DP2-PLXNA4/Be tetramer (PE-labeled). Each antigen-specific TCR was subsequently expressed as transfectomas for subsequent analyses. (B) Representative staining of T cell transfectomas with the HLA-DP2-PLXNA4/Be tetramer is shown. (C) Dose-response curves to PLXNA4 peptide were completed on the 4 murine-derived T cell transfectomas and human transfectoma AV22 for comparison. Various amounts of peptide (0.1 nM – 10 μM) and 75 μM $BeSO_4$ were added to wells containing equal numbers of transfectoma cells and DP2.21 fibroblasts. IL-2 secretion (pg/ml) was measured by ELISA after 22 hours of culture, and data are plotted as the percentage of maximum IL-2 against peptide concentration in the presence of $BeSO_4$. $EC_{50}$ values (nM) are shown, and results are representative of three independent experiments.

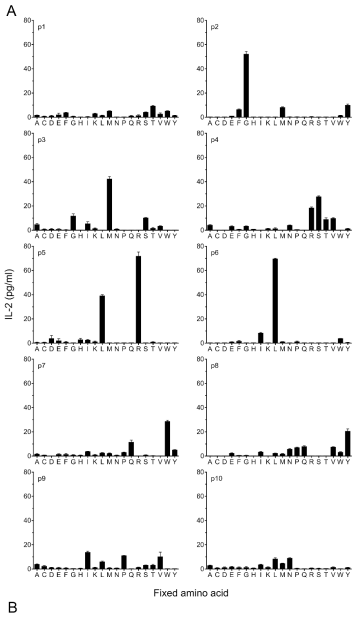


B

| Net IL-2 | Amino acid position | | | | | | | | | |
|---|---|---|---|---|---|---|---|---|---|---|
| | 1 | 2 | 3 | 4 | 5 | 6 | 7 | 8 | 9 | 10 |
| >40 pg/ml | | **G** | **M** | | **R** | **L** | | | | |
| 20-40 pg/ml | | | | **S** | **L** | | **W** | **Y** | | |
| 10-20 pg/ml | Y | G<br>S | | **R** | | | **Q** | | **I**<br>P<br>V | |
| 5-10 pg/ml | **T**<br>M<br>W | M | | V<br>T | | Y | Q<br>V<br>P<br>N | L | **L**<br>N | |

**Figure 7.**

Response of T cell transfectoma LB9-18 to 200 mixtures of decapeptide positional scanning library TPIMS 2040 in the presence of $BeSO_4$ (75 μM). (A) At each position of the peptide (p1 to p10, see histograms), individual mixtures were composed of peptides having one defined amino acid (20 amino acids, labeled on x-axis in single letter code) and randomized amino acids at the remaining 9 peptide positions. T cell transfectoma activation was assessed by IL-2 secretion (ELISA) after overnight culture of transfectoma cells with mixtures (200 μg/ml) and $BeSO_4$, presented by DP2.21 cells in protein-free media. A positive IL-2 response to particular mixtures demonstrates the presence of active peptides within the mixture and provides insight into which amino acids are preferred at a given position of the peptide. Data show IL-2 (mean ± SEM) of three separate experiments done in duplicate. IL-2 produced in wells not containing mixtures was below limits of detection. (B) Summary of the most active mixtures from positional scanning library TPIMS 2040. Mixtures were grouped by their ability to stimulate transfectoma LB9-18 by determining net IL-2 secretion (subtracting the amount of IL-2 secreted in wells not containing mixtures from IL-2 values obtained from wells that included mixtures). Bolded amino acids indicated those that were chosen for the generation of mimotopes.

A

| Mimotope | Peptide Sequence | | | | | | | | | | LB9-18 | | |
|---|---|---|---|---|---|---|---|---|---|---|---|---|---|
| | 1 | 2 | 3 | 4 | 5 | 6 | 7 | 8 | 9 | 10 | 50 µg/ml | 5.0 µg/ml | 0.5 µg/ml |
| 6 | F | G | M | S | R | L | W | Y | I | L | 845 | 1174 | 402 |
| 5 | T | G | M | S | R | L | W | Y | I | L | 816 | 887 | 42 |
| 13 | F | G | M | R | R | L | W | Y | I | L | 749 | 276 | 53 |
| 7 | T | G | M | S | R | L | Q | Y | I | L | 457 | 27 | - |
| 9 | F | G | M | R | L | L | W | Y | I | L | 372 | 18 | - |
| 1 | T | G | M | S | L | L | W | Y | I | L | 17 | - | - |
| 2 | F | G | M | S | L | L | W | Y | I | L | - | - | - |
| 3 | T | G | M | S | L | L | Q | Y | I | L | - | - | - |
| 4 | F | G | M | S | L | L | Q | Y | I | L | - | - | - |
| 8 | T | G | M | R | L | L | W | Y | I | L | - | - | - |
| 10 | T | G | M | R | L | L | Q | Y | I | L | - | - | - |
| 11 | F | G | M | R | L | L | Q | Y | I | L | - | - | - |
| 12 | T | G | M | R | R | L | W | Y | I | L | - | - | - |
| 14 | T | G | M | R | R | L | Q | Y | I | L | - | - | - |

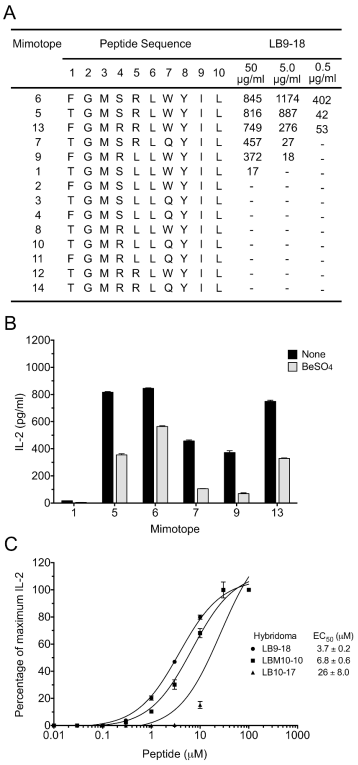


**Figure 8.**

Be-specific T cell transfectomas recognize mimotopes in a Be-independent manner. (A) The sequence of each mimotope was based on the results of the decapeptide positional scanning for LB9-18. Equal numbers of LB9-18 cells and DP2.21 antigen-presenting cells were mixed with crude preparations of mimotopes (0.5, 5.0 and 50 µg/ml) and $BeSO_4$ (75 µM). IL-2 secretion was measured by ELISA after 22 hours of culture. Mimotopes are ordered by LB9-18 response to 50 µg/ml of peptide. Hyphens indicate no IL-2 secretion above background levels in response to mimotope. (B) T cell transfectoma LB9-18 response to select mimotopes in the presence and absence of $BeSO_4$ (75 µM) is shown. Data are plotted as mean IL-2 secretion (pg/ml) for each mimotope. (C) Shown are dose-response curves for T cell transfectomas LB9-18, LBM10-10 and LB10-17 to highly purified (>95%) mimotope 6 peptide. Data are plotted as the percentage of maximum IL-2 secretion against peptide. $EC_{50}$ values (µM) for each transfectoma are shown, and data are representative of three independent experiments.

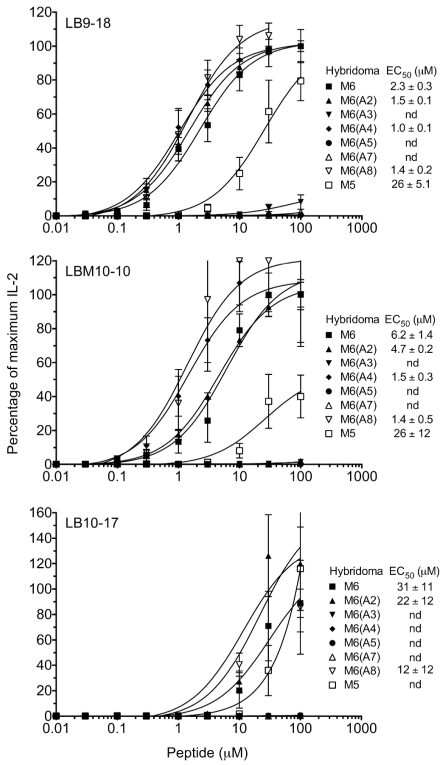


**Figure 9.**

Be-specific T cell transfectoma response to alanine substitutions of mimotope-6. Peptide dose-response curves were completed for T cell transfectomas LB9-18, LBM10-10 and LB10-17. Equal numbers of T cell transfectoma cells and DP2.21 antigen-presenting cells were mixed with $BeSO_4$ (75 μM) and highly purified peptides with single alanine-substitutions at positions 2, 3, 4, 5, 7, and 8 of mimotope-6. IL-2 secretion was measured by ELISA after 22 hours of culture, and data are plotted as the percentage of maximum IL-2 secretion against peptide concentration in the presence of $BeSO_4$. $EC_{50}$ values (mean ± SEM μM) for mimotope-6 and each variant peptide from four independent experiments are shown. nd: not determined.